GEOLOGY | THE GEOLOGICAL SOCIETY OF AMERICA®

https://doi.org/10.1130/G50344.1

Manuscript received 22 April 2022
Revised manuscript received 1 August 2022
Manuscript accepted 2 September 2022

Published online 2 December 2022

Chromium isotopes track redox fluctuations in Proterozoic successions of the Chapada Diamantina, São Francisco craton, Brazil

Fabrício A. Caxito[1], Robert Frei[2], Alcides N. Sial[3], Gabriel J. Uhlein[1], William Alexandre Lima de Moura[1], Egberto Pereira[4] and René Rodrigues[4]

[1]CPMTC Research Center and Postgraduate Program in Geology, Universidade Federal de Minas Gerais, Belo Horizonte, 31270–901 Brazil

[2]Department of Geoscience and Natural Resource Management, University of Copenhagen, Øster Voldgade 10, 1350 Copenhagen, Denmark

[3]Núcleo de Estudos Geoquímicos–Laboratório de Isótopos Estáveis (NEG-LABISE), Universidade Federal de Pernambuco, Recife, 50670-901, Brazil

[4]Department of Stratigraphy and Paleontology, Universidade do Estado do Rio de Janeiro, Rio de Janeiro, 20550-019 Brazil

ABSTRACT

The Chapada Diamantina region in the São Francisco craton of eastern Brazil is composed of sedimentary successions containing both Mesoproterozoic and Neoproterozoic carbonate levels, making it a key natural laboratory for understanding the fluctuations of Earth's biogeochemical cycles during its middle age. The ca. 1.4–1.2 Ga Caboclo Formation stromatolites yielded unfractionated $\delta^{53}Cr_{auth}$ (authigenic) (~−0.54‰ to +0.08‰). Ediacaran cap carbonates and phosphatic stromatolites of the Salitre Formation, on the other hand, yielded fractionated $\delta^{53}Cr_{auth}$ reaching as high as +0.51‰, suggesting the input of ^{53}Cr-rich Cr(VI), first delivered through meltwater-induced post–snowball Earth fluctuating redox conditions and then through weathering and mobilization under a fully oxygenated environment. The acquired data set highlights the very distinct redox conditions throughout the Proterozoic and reinforces the suggestion that after the Cryogenian global glaciations, Earth's atmosphere and hydrosphere became progressively oxygenated during the Ediacaran-Cambrian transition.

INTRODUCTION

Multiple sedimentary, isotopic, and geochemical proxies suggest that Earth's atmospheric oxygen levels evolved through putative steps from an original anoxic Archean atmosphere, first during the Great Oxidation Event at ca. 2.4 Ga and then through a new protracted rise during the late Ediacaran, followed by the explosive diversification of complex life during the Precambrian-Cambrian transition (e.g., Lyons et al., 2014). The study of ancient chemical sedimentary rocks can provide useful insights on how Earth's biogeochemical cycles, paleogeographic and paleotectonic settings, and atmospheric and oceanic chemical conditions evolved and interacted with each other during the oxygenation events in the history of the planet and also during the dormant stages between those major putative steps. In this scenario, chromium isotopes emerged as a powerful tool for unraveling ancient atmospheric redox conditions because the Cr(VI) species, which is mobile under oxygenated weathering in reactions catalyzed by the presence of manganese oxides, is enriched in the ^{53}Cr isotope compared to the immobile Cr(III) species (Frei et al., 2011, 2009; Planavsky et al., 2014; Cole et al., 2016; Gilleaudeau et al., 2016; Canfield et al., 2018).

The Chapada Diamantina region in the São Francisco craton of eastern Brazil (Fig. 1) is an ideal place to unravel Proterozoic biogeochemical patterns because it is composed of shallow marine and continental rift-sag sedimentary successions containing both Mesoproterozoic (the ca. 1.4–1.2 Ga Caboclo Formation; Figs. 2A–2D) and Neoproterozoic (the Ediacaran phosphate-bearing Salitre Formation covering the Bebedouro Formation diamictites; Figs. 2E–2I) carbonate levels that can act as faithful recorders of seawater chemistry during precipitation (Frei et al., 2011). We investigate the Cr isotope signatures of those rocks along with novel trace element, Sr, C, and O isotope data (see the Supplemental Material[1]).

GEOLOGICAL SETTING

The São Francisco craton of eastern Brazil (Fig. 1) and its African counterpart, the Congo craton, consist of Archean nuclei bounded by Proterozoic orogenic belts (Heilbron et al., 2017). The main orogenic phase, at ca. 2.0–2.2 Ga, generated the major cratonic landmass and was followed by installation of widespread rift-sag basins (Guadagnin and Chemale, 2015).

The Chapada Diamantina Group was deposited in the central portion of the São Francisco craton ca. 1.8 to ca. 1.0 Ga, comprising a predominantly siliciclastic succession with continental and shallow marine sediments, in addition to felsic volcanics and volcaniclastics (e.g., Guadagnin and Chemale, 2015). One of the most important shallow marine levels within this package is the mixed siliciclastic-carbonate Caboclo Formation, representing a transgression over the continental Tombador Formation (Fig. 1). The latter contains crystal tuffs dated at ca. 1.4 Ga (Guadagnin et al., 2015), and both units contain youngest detrital zircons in the same age

[1]Supplemental Material. Materials and methods, Table S1 (isotope data), and Table S2 (trace element data). Please visit https://doi.org/10.1130/GEOL.S.21391212 to access the supplemental material, and contact editing@geosociety.org with any questions.

CITATION: Caxito, F.A., et al., 2023, Chromium isotopes track redox fluctuations in Proterozoic successions of the Chapada Diamantina, São Francisco craton, Brazil: Geology, v. 51, p. 69–74, https://doi.org/10.1130/G50344.1

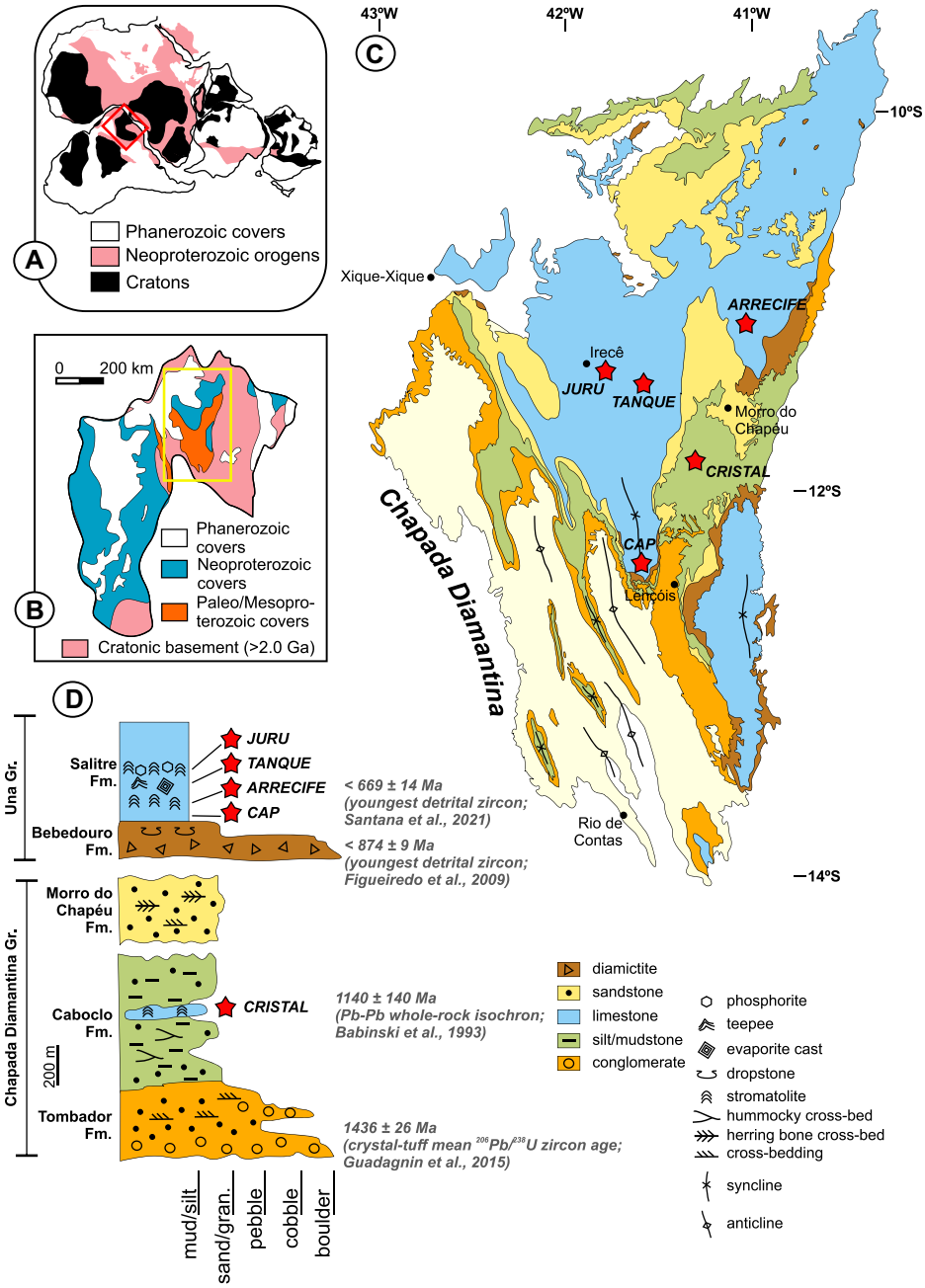

Figure 1. Chapada Diamantina region, eastern Brazil, in context of Gondwana (A) and São Francisco craton (B), with schematic map (C) and stratigraphic section (D) showing location of studied sections (red stars). Fm.—Formation; Gr.—Group; gran.—granule.

range (Guadagnin and Chemale, 2015). A Pb-Pb whole-rock isochron of 1140 ± 140 Ma on carbonate samples (Babinski et al., 1993) is, despite the high uncertainty and the caveats of interpretation of Pb-Pb whole-rock isochrons (which might be reset by post-depositional fluid percolation and/or incorporate Pb from basement-derived fluids), the only available minimum age constraint for the Caboclo Formation.

Stratigraphy and sedimentology of the Cristal cave, studied in this work, was detailed by Ferronatto et al. (2021). According to the authors, the site preserves offshore to shoreface facies, with carbonate-siliciclastic sediments and stromatolites occurring in all lithofacies associations. A low-gradient ramp dominated by normal and storm waves was proposed, with the absence of mud and predators allowing for widespread colonization by microbial communities in both shallow and deeper-water settings.

The top of the Chapada Diamantina Group is truncated by an erosional unconformity, above which glacial diamictites and related facies containing dropstones and striated clasts of the Bebedouro Formation were deposited (Guimarães et al., 2011), with youngest detrital zircons at ca. 874 Ma (Figueiredo et al., 2009). Atop the Bebedouro Formation, the Salitre Formation comprises a typical Neoproterozoic cap carbonate succession. Basal mudstones preserving negatively fractionated $\delta^{13}C$ ~−4.0‰ (all values relative to Vienna Peedee belemnite) are followed by domal and elongate digitate stromatolites, associated with economically important phosphatic cements and intraclasts, deposited in an energetic shallow platform environment with wave-swept microbial buildups (Misi and Veizer, 1998; Sanders and Grotzinger, 2021; Santana et al., 2021), with $\delta^{13}C$ ~0‰. Those are capped, ~300 m upsection, by dark, organic-rich oolitic limestone with $\delta^{13}C$ ~+9‰. The Bebedouro and Salitre Formations compose the Una Group.

Santana et al. (2021) recovered detrital zircons with a younger peak at 669 ± 14 Ma from putative tuffite beds within carbonates bearing $\delta^{13}C$ ~0‰ just above the cap carbonate. Although the authors interpreted the cap carbonate and associated glacial deposits as related to the mid-Cryogenian (717–660 Ma) Sturtian glaciation, the detrital zircon content is more coherently interpreted as indicating deposition during the Marinoan deglaciation, whose maximum onset time is constrained to ca. 657.17 ± 0.78 Ma, based on the U-Pb chemical abrasion–isotope dilution–thermal ionization mass spectrometry (CA-ID-TIMS) age of devitrified airfall ash deposits just below the Nantuo glacial deposits in China (Rooney et al., 2020). Interpretation of the Salitre Formation cap carbonate as related to the global post-Marinoan, early Ediacaran deglacial stage at ca. 635 Ma is followed by Misi and Veizer (1998) and Sanders and Grotzinger (2021). The latter compared the phosphorite deposits in the Salitre Formation and the Sete Lagoas Formation of the Ediacaran-Cambrian Bambuí Group on the southern São Francisco craton. The base of the Sete Lagoas Formation is marked by a cap carbonate succession of the Pedro Leopoldo Member. Exaragonite crystal fans preserved in limestone tens of meters above the basal cap dolostone yielded U-Pb laser ablation–inductively coupled plasma–mass spectrometry (LA-ICPMS) ages of 615–608 Ma (Caxito et al., 2021).

An age span between 635 and 600 Ma for deposition of the cap carbonate succession is coherent with data from other successions, as illustrated by sensitive high-resolution ion microprobe (SHRIMP) and CA-ID-TIMS tuff U-Pb dates of 614 ± 8 Ma (Liu et al., 2009) and 612.5 ± 0.9 Ma (Yang et al., 2021), respectively, ~20 and 40 m above the base of the Doushantuo Formation in platformal settings of South China, interleaved in carbonates within the negative $\delta^{13}C$ excursion associated with the post-Marinoan excursion. These data suggest that while deposition of the basal cap dolostone was probably fast ca. 635 Ma, as bracketed by several CA-ID-TIMS U-Pb zircon data from ash fall tuffs (Hoffmann et al., 2004; Condon et al.,

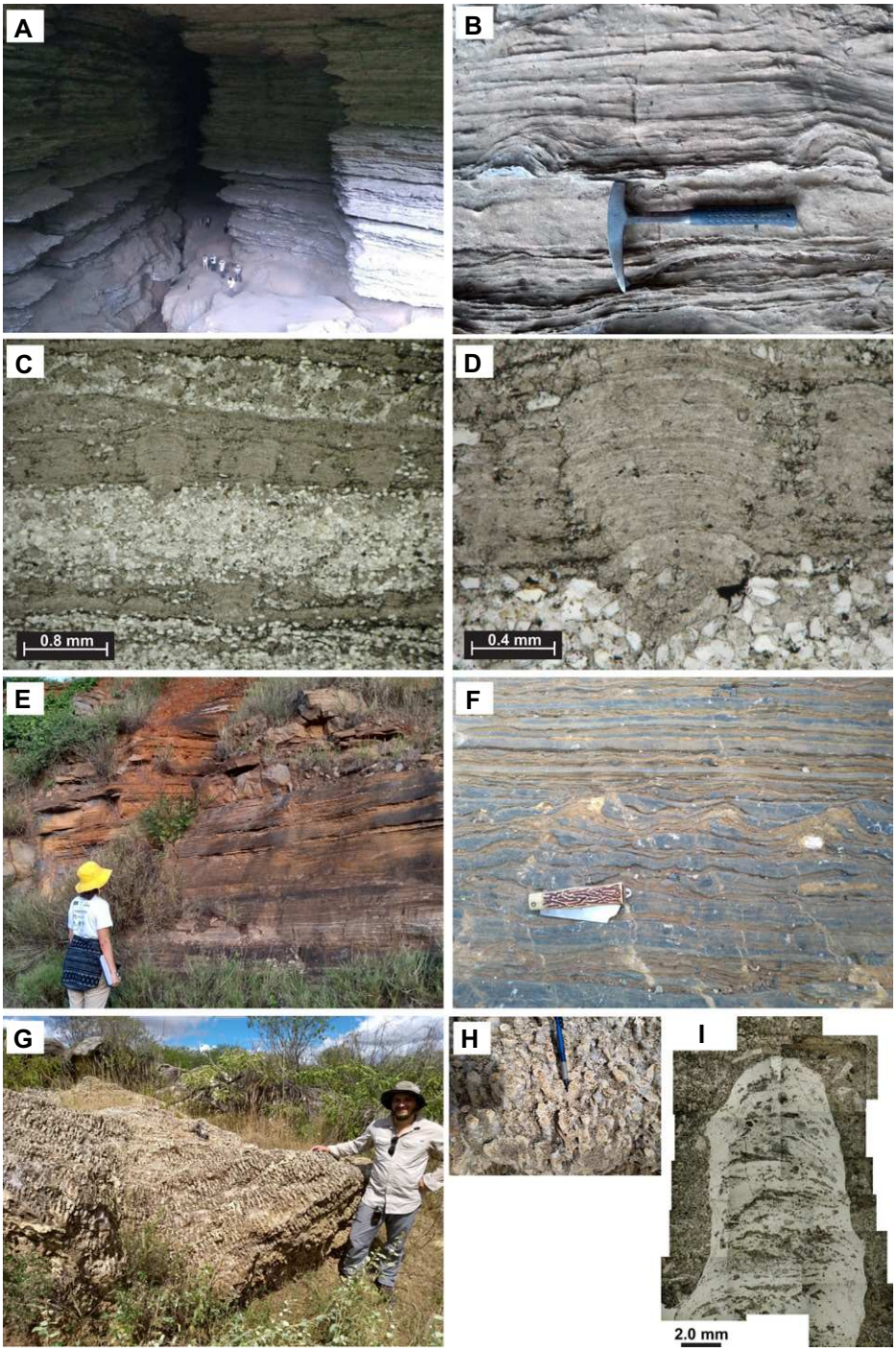

Figure 2. Field (A, B, E–H) and thin-section (C, D, I; under uncrossed polarizers) photos of studied outcrops and samples. (A–D) Ectasian–Stenian Caboclo Formation stromatolitic limestones in Cristal cave (A), stromatolitic mounds (B), and detail in thin section (C,D). (E–I) Early Ediacaran Salitre Formation cap carbonate (Cap section) (E), pseudo-teepee structures in limestone of Tanque section (F), columnar phosphatic *Jurusania krilov* (Srivastava, 1982) stromatolites (Juru section) (G,H), and mosaic of *Jurusania krilov* column on thin section (I).

2005; Calver et al., 2013; Prave et al., 2016) as well as Re-Os data (Rooney et al., 2015) from various glacially related units worldwide, deposition of the aragonite fan–bearing limestone above it could have spanned tens of millions of years.

The Salitre Formation presents $^{87}Sr/^{86}Sr$ and $\delta^{13}C$ data sets identical to those of the Bambuí Group (Caxito et al., 2021). A sharp peak in $^{87}Sr/^{86}Sr$ in the basal negative-$\delta^{13}C$, high-[Sr], and relatively high-$\delta^{18}O$ (mostly −5‰ to −6‰) limestones, from ~0.7078 to 0.7084 (Misi and Veizer, 1998; Caxito et al., 2021), is similar to that of other post-Marinoan cap carbonates globally and probably registers enhanced continental weathering due to high pCO_2 in the aftermath of the end-Cryogenian glaciation (Halverson et al., 2007).

Upsection, in both the Bambuí and Una Groups, $^{87}Sr/^{86}Sr$ values progressively decrease, reaching ~0.7075 in the terminal blackish limestones that preserve (in other sections of the Salitre Formation, not studied here) highly positive $\delta^{13}C$ (Misi and Veizer, 1998). The decoupling of $\delta^{13}C$ and $^{87}Sr/^{86}Sr$ values from the global seawater curve in the middle to upper portion of both units is interpreted as due to basin restriction in the late Ediacaran to Cambrian as the São Francisco craton became progressively surrounded by the Brasiliano mountain belts that were the culmination of western Gondwana assembly (Caxito et al., 2021). Thus, while the basal cap carbonate unit of the Salitre Formation would correspond to the Pedro Leopoldo cap carbonate at ca. 635–600 Ma, the phosphatic stromatolites and the topmost black limestones that occur in other sections of the Salitre Formation would correspond to the Lagoa Santa Member of the Sete Lagoas Formation, preserving blackish stromatolites with $\delta^{13}C$ as high as ~+10‰ and probably deposited ca. 580–550 Ma, according to U-Pb in situ carbonate LA-ICPMS dating (Caxito et al., 2021).

RESULTS

Trace element and C, O, Sr, and Cr isotope data (Figs. 3 and 4; Tables S1 and S2 in the Supplemental Material) were obtained according to the procedures described in the Supplemental Material. Cross-plots of $\delta^{53}Cr_{meas}$ (measured) with proxies for detrital contamination such as Al, Zr, Ti, and Sc (Fig. 4) are generally scattered, suggesting a good approximation to the original chemical precipitates. The data discussed below and presented in Figure 3 correspond to $\delta^{53}Cr_{auth}$ (authigenic) calculated using the correction for detrital Cr with Al as a proxy for detrital contamination, after Gilleaudeau et al. (2018).

Sixteen (16) samples of the Caboclo Formation from the Cristal cave yielded $\delta^{13}C$ in a narrow range of −2.1‰ to −1.2‰ (with an outlier of −4.5‰), with associated $\delta^{18}O$ of −9.4‰ to −6.8‰ and unfractionated $\delta^{53}Cr_{auth}$ of −0.21‰ to +0.08‰, with an outlier of −0.54‰ (Table S1). Most samples show slightly middle rare earth element (MREE)–enriched post-Archean Australian shale (PAAS)–normalized patterns (Fig. 4A), with Y/Ho ratios between 29 and 40. Ce/Ce* values are generally >0.9 except for two outliers at 0.77 and 0.85, and Eu/Eu* values are 0.85–1.78 with an outlier of 3.98. Sr concentrations are very low, < 30 ppm, and thus $^{87}Sr/^{86}Sr$ ratios do not reflect the original seawater composition.

Samples from four different sections of the Ediacaran Salitre Formation were studied. The basal cap carbonate (Cap section) yielded $\delta^{13}C$ from −2.9‰ to −0.4‰, with associated $\delta^{18}O$ ~−8‰ and $\delta^{53}Cr_{auth}$ of −0.12‰ to +0.17‰.

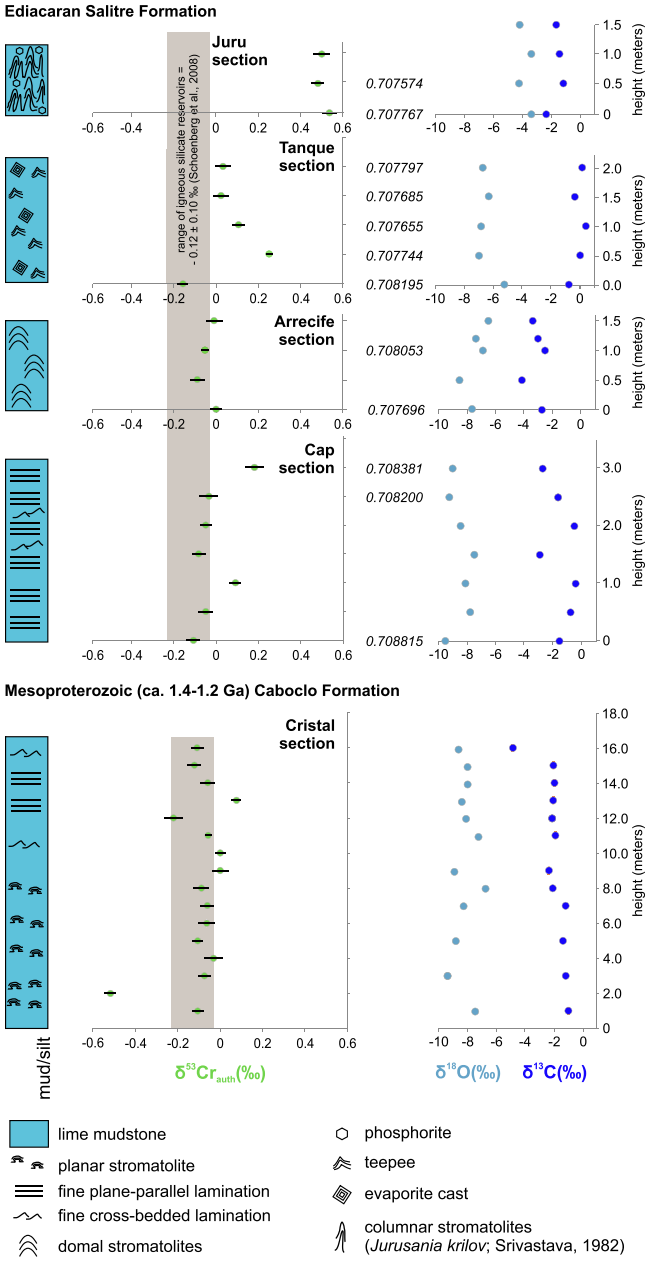

Figure 3. Isotope stratigraphy data for studied sections. Errors bars represent the analytical uncertainty in Cr isotope data. Italics represent least-radiogenic $^{87}Sr/^{86}Sr$ for samples with [Sr] > 300 ppm. auth—authigenic.

Slightly MREE + Y–enriched patterns with associated Y/Ho ratios of 26–29, Ce/Ce* of 0.77–0.96, and Eu/Eu* of 0.73–1.01 characterize the samples. The samples with higher Sr concentrations, > 387 ppm, yielded $^{87}Sr/^{86}Sr$ ratios of 0.7082–0.7088.

Samples from the Arrecife farm domal stromatolites (Arrecife section) also yielded negatively fractionated $\delta^{13}C$ from −4.1‰ to −2.5‰, with associated $\delta^{18}O$ of −6.5‰ to −8.5‰ and fairly unfractionated $\delta^{53}Cr_{auth}$ of −0.08‰ to 0‰. PAAS-normalized rare earth element (REE) + Y patterns are relatively flat with only slight MREE enrichment, with associated Y/Ho ratios of 28–33, Ce/Ce* of 0.94–0.98, and Eu/Eu* of 0.85–1.09. Two samples with Sr concentration of 371 and 1585 ppm yielded $^{87}Sr/^{86}Sr$ ratios of 0.7081 and 0.7077, respectively.

Carbonate samples from the Tanque farm (Tanque section), containing teepee and evaporite cast structures, yielded $\delta^{13}C$ of −0.12‰ to +0.23‰, with $\delta^{18}O$ ~−6‰ and positively fractionated $\delta^{53}Cr_{auth}$ as high as +0.25‰. REE + Y patterns are relatively flat. Y/Ho ratios are 29–32, Ce/Ce* values are 0.95–1.03, and Eu/Eu* values are 0.86–1.07. All samples are Sr rich (437–2291 ppm) and show $^{87}Sr/^{86}Sr$ between 0.7077 and 0.7082.

Finally, samples from the phosphatic interdigitate stromatolites (Juru section) yielded $\delta^{13}C$ of −2.3‰ to −1.2‰, $\delta^{18}O$ ~−3.5‰, and the most positively fractionated $\delta^{53}Cr_{auth}$ of to +0.45‰ to +0.51‰. PAAS-normalized REE + Y patterns show depletion of light REEs (LREEs) and pronounced positive Y anomalies with Y/Ho of 40–44, with associated Ce/Ce* of 1.16–1.19 and Eu/Eu* of 0.95–1.11. Two samples with Sr concentrations of 431 and 607 ppm yielded $^{87}Sr/^{86}Sr$ of 0.7076 and 0.7078, respectively.

DISCUSSION AND CONCLUSIONS

The data obtained are coherent with current interpretations that suggest widely distinct redox conditions throughout the Proterozoic. Although fractionated $\delta^{53}Cr$ values were reported from Mesoproterozoic-aged shales dating back to 1350 Ma in the Shennongjia Group of South China (Canfield et al., 2018), data compilations using ironstones and shales (Cole et al., 2016; Planavsky et al., 2014) reveal a general lack of fractionation in the 1600–1000 Ma interval. Marine carbonates record the first whiffs of a renewed oxygenation pulse at 1112–970 Ma (Gilleaudeau et al., 2016).

The Caboclo Formation depositional age is roughly constrained between ca. 1.4 (younger detrital zircon population; Guadagnin and Chemale, 2015) and ca. 1.2 Ga (Pb-Pb whole-rock isochron; Babinski et al., 1993), thus fitting the above-discussed intervals and probably representing an Ectasian–Stenian carbonate-siliciclastic ramp. The lack of positive chromium isotope fractionation suggests that oxidative weathering was not important at the time of deposition, and the general lack of negative values below the mean values of the common lithogenic reservoirs (except for one sample) suggests that microbially induced fractionation was not a major factor as well (Uhlein et al., 2021).

The Ediacaran Salitre Formation carbonates, on the other hand, show positively fractionated $\delta^{53}Cr_{auth}$ values, attaining maximum values ~+0.5‰ in the phosphate-bearing interdigitate stromatolites (Table S1). The cap carbonate *sensu stricto*, sitting immediately atop glacial diamictites, preserves only minor fractionation, with most values plotting within the lithogenic reservoir range. These data are consistent with $\delta^{53}Cr_{auth}$ fluctuations (Rodler et al., 2016a, 2016b; Caxito et al., 2018) and other proxies such as Ce anomalies, iron speciation data, and redox-sensitive elements (Hippertt et al., 2019) for other basal Ediacaran cap carbonates around the world, suggesting unstable redox conditions marked by protracted oceanic and possibly atmospheric oxygenation (Rodler et al., 2016a, 2016b; Caxito et al., 2018).

Higher in the carbonate succession, the association of phosphorites with consistently positively fractionated Cr isotope ratios suggest broad oxygenated conditions and high bioavailability of phosphorus, setting the stage for the colonization of benthic metazoans and biomineralizing biota under balanced redox and nutrient conditions and triggering higher-style trophic chains due to ecological innovations made possible by higher oxygen levels, such as

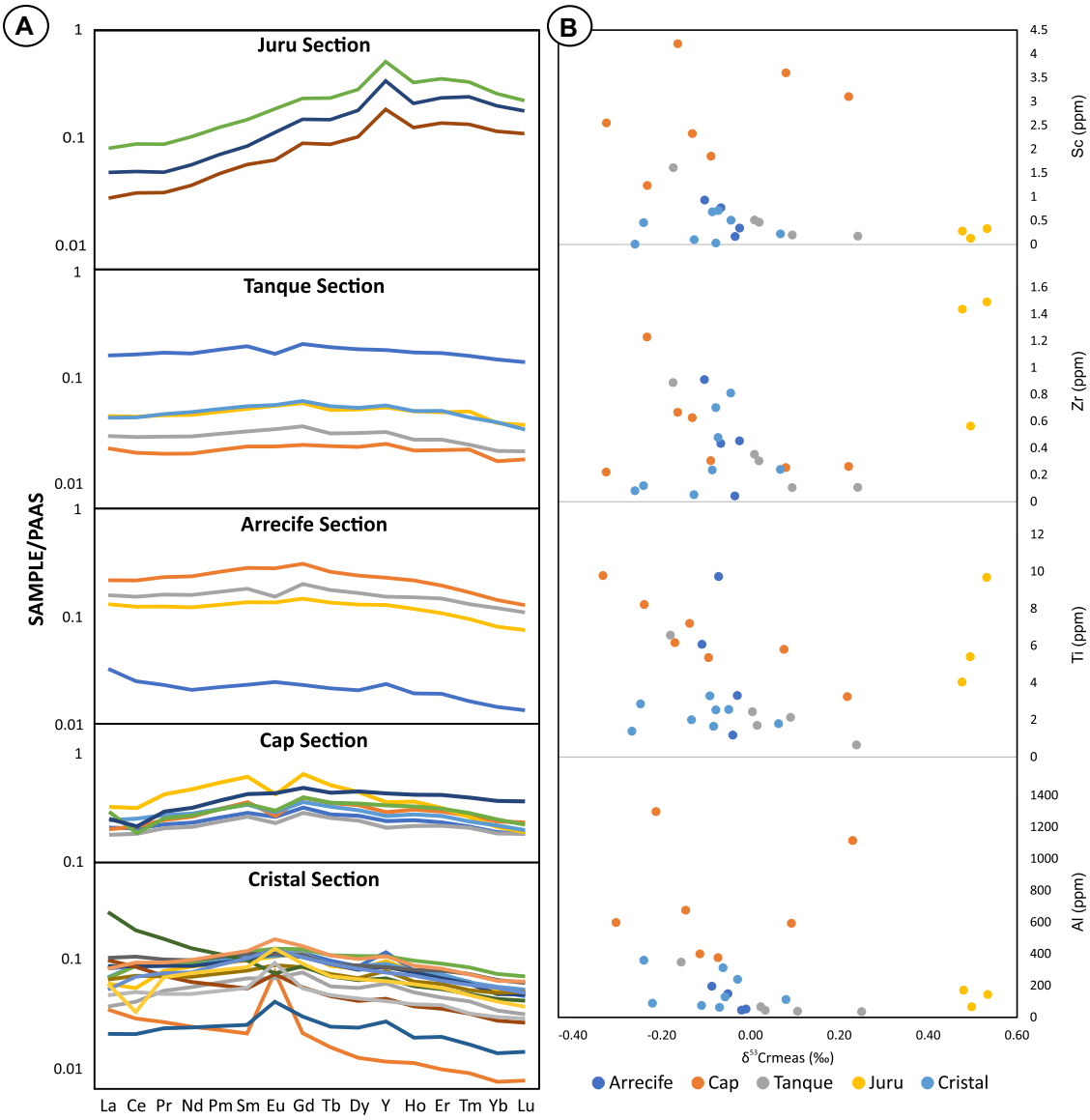

Figure 4. Trace element data for studied sections. (A) Post-Archean Australian shale (PAAS)–normalized rare earth elements + Y data. (B) Cross-plots of proxies for detrital influence versus measured $\delta^{53}Cr$ ($\delta^{53}Cr_{meas}$).

predation and motility (Sperling et al., 2013). Late Ediacaran macrofossils were, however, not yet found in the Salitre Formation. Although conditions of relatively high oxygen fugacity might have been attained, it is interesting to notice that the highest $\delta^{53}Cr_{auth}$ values occur in the interval with the highest $\delta^{18}O$ values of the data set (Juru section, ~−4‰). This might indicate higher rates of evaporation and the development of a restricted and shallow hypersaline environment, which would have been suitable for mat-building microorganisms but probably deadly for Ediacaran macrobiota.

ACKNOWLEDGMENTS

This work is supported by Instituto Serrapilheira (Serra-1912-31510), Brazil, through Project MOBILE (www.geolifemobile.com); by FAPEMIG, Brazil, through the "Programa Pesquisador Mineiro" (PPM-00618-18); and by the Conselho Nacional de Desenvolvimento Científico e Tecnológico (CNPq), Brazil, through grant 408815/2021-3 and through Research Productivity Grant 304509/2021-3 to Caxito. A previous version was improved after comments and suggestions of two anonymous reviewers.

REFERENCES CITED

Babinski, M., Van Schmus, W.R., Chemale, F., Jr., Brito Neves, B.B., and Rocha, A.J.D., 1993, Idade isocrônica Pb/Pb em rochas carbonáticas da Formação Caboclo, em Morro do Chapéu, BA, *in* Pedreira, A et al., eds., II Simpósio Sobre o Cráton do São Francisco: Evolução Tectônica e Metalogenética, 2: Salvador, Brazil, Sociedade Brasileira de Geologia, p. 160–163.

Calver, C.R., Crowley, J.L., Wingate, M.T.D., Evans, D.A.D., Raub, T.D., and Schmitz, M.D., 2013, Globally synchronous Marinoan deglaciation indicated by U-Pb geochronology of the Cottons Breccia, Tasmania, Australia: Geology, v. 41, p. 1127–1130, https://doi.org/10.1130/G34568.1.

Canfield, D.E., Zhang, S.C., Frank, A.B., Wang, X.M., Wang, H.J., Su, J., Ye, Y.T., and Frei, R., 2018, Highly fractionated chromium isotopes in Mesoproterozoic-aged shales and atmospheric oxygen: Nature Communications, v. 9, 2871, https://doi.org/10.1038/s41467-018-05263-9.

Caxito, F.A., Frei, R., Uhlein, G.J., Gonçalves Dias, T., Árting, T.B., and Uhlein, A., 2018, Multiproxy geochemical and isotope stratigraphy records of a Neoproterozoic Oxygenation Event in the Ediacaran Sete Lagoas cap carbonate, Bambuí Group, Brazil: Chemical Geology, v. 481, p. 119–132, https://doi.org/10.1016/j.chemgeo.2018.02.007.

Caxito, F., et al., 2021, Goldilocks at the dawn of complex life: Mountains might have damaged Ediacaran–Cambrian ecosystems and prompted an early Cambrian greenhouse world: Scientific Reports, v. 11, 20010, https://doi.org/10.1038/s41598-021-99526-z.

Cole, D.B., Reinhard, C.T., Wang, X.L., Gueguen, B., Halverson, G.P., Gibson, T., Hodgskiss, M.S.W., McKenzie, N.R., Lyons, T.W., and Planavsky, N.J., 2016, A shale-hosted Cr isotope record of low atmospheric oxygen during the Proterozoic: Geology, v. 44, p. 555–558, https://doi.org/10.1130/G37787.1.

Condon, D., Zhu, M.Y., Bowring, S., Wang, W., Yang, A.H., and Jin, Y.G., 2005, U-Pb ages from the Neoproterozoic Doushantuo Formation, China: Science, v. 308, p. 95–98, https://doi.org/10.1126/science.1107765.

Ferronatto, J.P.F., Scherer, C.M.d.S., Drago, G.B., Rodrigues, A.G., de Souza, E.G., dos Reis, A.D., Bállico, M.B., Kifumbi, C., and Cazarin, C.L., 2021, Mixed carbonate-siliciclastic sedimentation in a Mesoproterozoic storm-dominated

ramp: Depositional processes and stromatolite development: Precambrian Research, v. 361, 106240, https://doi.org/10.1016/j.precamres.2021.106240.

Figueiredo, F.T., de Almeida, R.P., Tohver, E., Babinski, M., Liu, D.Y., and Fanning, C.M., 2009, Neoproterozoic glacial dynamics revealed by provenance of diamictites of the Bebedouro Formation, São Francisco Craton, Central Eastern Brazil: Terra Nova, v. 21, p. 375–385, https://doi.org/10.1111/j.1365-3121.2009.00893.x

Frei, R., Gaucher, C., Poulton, S.W., and Canfield, D.E., 2009, Fluctuations in Precambrian atmospheric oxygenation recorded by chromium isotopes: Nature, v. 461, p. 250–253, https://doi.org/10.1038/nature08266.

Frei, R., Gaucher, C., Døssing, L.N., and Sial, A.N., 2011, Chromium isotopes in carbonates—A tracer for climate change and for reconstructing the redox state of ancient seawater: Earth and Planetary Science Letters, v. 312, p. 114–125, https://doi.org/10.1016/j.epsl.2011.10.009.

Gilleaudeau, G.J., Frei, R., Kaufman, A.J., Kah, L.C., Azmy, K., Bartley, J.K., Chernyavskiy, P., and Knoll, A.H., 2016, Oxygenation of the mid-Proterozoic atmosphere: Clues from chromium isotopes in carbonates: Geochemical Perspectives Letters, v. 2, p. 178–187, https://doi.org/10.7185/geochemlet.1618.

Gilleaudeau, G.J., Voegelin, A.R., Thibault, N., Moreau, J., Ullmann, C.V., Klaebe, R.M., Korte, C., and Frei, R., 2018, Stable isotope records across the Cretaceous-Paleogene transition, Stevns Klint, Denmark: New insights from the chromium isotope system: Geochimica et Cosmochimica Acta, v. 235, p. 305–332, https://doi.org/10.1016/j.gca.2018.04.028.

Guadagnin, F., and Chemale, F., Jr., 2015, Detrital zircon record of the Paleoproterozoic to Mesoproterozoic cratonic basins in the São Francisco Craton: Journal of South American Earth Sciences, v. 60, p. 104–116, https://doi.org/10.1016/j.jsames.2015.02.007.

Guadagnin, F., Chemale, F., Jr., Magalhães, A.J.C., Santana, A., Dussin, I., and Takehara, L., 2015, Age constraints on crystal-tuff from the Espinhaço Supergroup—Insight into the Paleoproterozoic to Mesoproterozoic intracratonic basin cycles of the Congo–São Francisco Craton: Gondwana Research, v. 27, p. 363–376, https://doi.org/10.1016/j.gr.2013.10.009.

Guimarães, J.T., Misi, A., Pedreira, A.J., and Dominguez, J.M.L., 2011. The Bebedouro Formation, Una Group, Bahia (Brazil), *in* Arnaud, E., et al., eds., The Geological Record of Neoproterozoic Glaciations: Geological Society, London, Memoir 36, p. 503–508, https://doi.org/10.1144/M36.47

Halverson, G.P., Dudás, F.Ö., Maloof, A.C., and Bowring, S.A., 2007, Evolution of the $^{87}Sr/^{86}Sr$ composition of Neoproterozoic seawater: Palaeogeography, Palaeoclimatology, Palaeoecology, v. 256, p. 103–129, https://doi.org/10.1016/j.palaeo.2007.02.028.

Heilbron, M., Cordani, U.G., and Alkmim, F.F., eds., 2017, São Francisco Craton, Eastern Brazil: Tectonic Genealogy of a Miniature Continent: Cham, Switzerland, Springer International Publishing, 331 p., https://doi.org/10.1007/978-3-319-01715-0

Hippertt, J.P., Caxito, F.A., Uhlein, G.J., Nalini, H.A., Sial, A.N., Abreu, A.T., and Nogueira, L.B., 2019, The fate of a Neoproterozoic intracratonic marine basin: Trace elements, TOC and IRON speciation geochemistry of the Bambuí Basin, Brazil: Precambrian Research, v. 330, p. 101–120, https://doi.org/10.1016/j.precamres.2019.05.001.

Hoffmann, K.H., Condon, D.J., Bowring, S.A., and Crowley, J.L., 2004, U-Pb zircon date from the Neoproterozoic Ghaub Formation, Namibia: Constraints on Marinoan glaciation: Geology, v. 32, p. 817–820, https://doi.org/10.1130/G20519.1.

Liu, P.J., Yin, C.Y., Gao, L.Z., Tang, F., and Chen, S.M., 2009, New material of microfossils from the Ediacaran Doushantuo Formation in the Zhangcunping area, Yichang, Hubei Province and its zircon SHRIMP U-Pb age: Chinese Science Bulletin, v. 54, p. 1058–1064, https://doi.org/10.1007/s11434-008-0589-6.

Lyons, T.W., Reinhard, C.T., and Planavsky, N.J., 2014, The rise of oxygen in Earth's early ocean and atmosphere: Nature, v. 506, p. 307-315, https://doi.org/10.1038/nature13068.

Misi, A., and Veizer, J., 1998, Neoproterozoic carbonate sequences of the Una Group, Irecê Basin, Brazil: Chemostratigraphy, age and correlations: Precambrian Research, v. 89, p. 87–100, https://doi.org/10.1016/S0301-9268(97)00073-9.

Planavsky, N.J., Reinhard, C.T., Wang, X.L., Thomson, D., McGoldrick, P., Rainbird, R.H., Johnson, T., Fischer, W.W., and Lyons, T.W., 2014. Low Mid-Proterozoic atmospheric oxygen levels and the delayed rise of animals: Science, v. 346, p. 635–638. https://doi.org/10.1126/science.1258410

Prave, A.R., Condon, D.J., Hoffmann, K.H., Tapster, S., and Fallick, A.E., 2016, Duration and nature of the end-Cryogenian (Marinoan) glaciation: Geology, v. 44, p. 631–634, https://doi.org/10.1130/G38089.1.

Rodler, A.S., Frei, R., Gaucher, C., and Germs, G.J.B., 2016a, Chromium isotope, REE and redox-sensitive trace element chemostratigraphy across the late Neoproterozoic Ghaub glaciation, Otavi Group, Namibia: Precambrian Research, v. 286, p. 234–249, https://doi.org/10.1016/j.precamres.2016.10.007.

Rodler, A.S., Hohl, S.V., Guo, Q., and Frei, R., 2016b, Chromium isotope stratigraphy of Ediacaran cap dolostones, Doushantuo Formation, South China: Chemical Geology, v. 436, p. 24–34, https://doi.org/10.1016/j.chemgeo.2016.05.001.

Rooney, A.D., Strauss, J.V., Brandon, A.D., and Macdonald, F.A., 2015, A Cryogenian chronology: Two long-lasting synchronous Neoproterozoic glaciations: Geology, v. 43, p. 459–462, https://doi.org/10.1130/G36511.1.

Rooney, A.D., Yang, C., Condon, D.J., Zhu, M.Y., and Macdonald, F.A., 2020, U-Pb and Re-Os geochronology tracks stratigraphic condensation in the Sturtian snowball Earth aftermath: Geology, v. 48, p. 625–629, https://doi.org/10.1130/G47246.1.

Sanders, C., and Grotzinger, J., 2021, Sedimentological and stratigraphic constraints on depositional environment for Ediacaran carbonate rocks of the São Francisco Craton: Implications for phosphogenesis and paleoecology: Precambrian Research, v. 363, 106328, https://doi.org/10.1016/j.precamres.2021.106328.

Santana, A., Chemale, F., Scherer, C., Guadagnin, F., Pereira, C., and Santos, J.O.S., 2021, Paleogeographic constraints on source area and depositional systems in the Neoproterozoic Irecê Basin, São Francisco Craton: Journal of South American Earth Sciences, v. 109, 103330, https://doi.org/10.1016/j.jsames.2021.103330.

Schoenberg, R., Zink, S., Staubwasser, M., and von Blanckenburg, F., 2008, The stable Cr isotope inventory of solid Earth reservoirs determined by double spike MC-ICP-MS: Chemical Geology, v. 249, p. 294–306.

Sperling, E.A., Frieder, C.A., Raman, A.V., Girguis, P.R., Levin, L.A., and Knoll, A.H., 2013, Oxygen, ecology, and the Cambrian radiation of animals: Proceedings of the National Academy of Sciences of the United States of America, v. 110, p. 13,446–13,451, https://doi.org/10.1073/pnas.1312778110.

Srivastava, N.K., 1982, Algumas observações sobre os estromatolitos dos Grupos Una (Bahia) e Vaza Barris (Sergipe), Nordeste do Brazil: Ciências da Terra, v. 3, p. 7–11.

Uhlein, G.J., Caxito, F.A., Frei, R., Uhlein, A., Sial, A.N., and Dantas, E.L., 2021, Microbially induced chromium isotope fractionation and trace elements behavior in lower Cambrian microbialites from the Jaíba Member, Bambuí Basin, Brazil: Geobiology, v. 19, p. 125–146, https://doi.org/10.1111/gbi.12426.

Yang, C., Rooney, A.D., Condon, D.J., Li, X.H., Grazhdankin, D.V., Bowyer, F.T., Hu, C. L., Macdonald, F.A., and Zhu, M.Y., 2021, The tempo of Ediacaran evolution: Science Advances, v. 7, eabi9643, https://doi.org/10.1126/sciadv.abi9643.

Printed in USA